The International Innovations Journal of Applied Science (IIJAS) Vol. 1, No.2, 15-09-2024
المجلد الأول العدد الثاني 15-9-2024 (IIJAS) مجلة ابتكارات الدولية للعلوم التطبيقية
https://doi.org/10.61856/6w30zq45

SCIENTIFIC EVENTS GATE

The International Innovations Journal of Applied Science

Journal homepage: https://iijas.eventsgate.org/iijas

ISSN: 3009-1853 Online

Recycling Agricultural Wastes for Controlled Drug Delivery Systems with DFT Calculations

Hebat-Allah S. Tohamy*[1]

[1]Cellulose and Paper Department, National Research Centre, 33 El Bohouth Str., P.O. 12622, Dokki Giza, Egypt

ARTICLE INFO

Article history:
Received 20 Feb. 2024,
Revised 21 May 2024,
Accepted 25 May 2024,
Available online 15 Sep. 2024

Keywords:
Graphene oxide
Carbon nanotubes
Agrowastes
Recycling
DFT
Sugarcane bagasse
Drug loading

ABSTRACT

To make these materials, we used a simple oven muffle furnace for heating the sugarcane bagasse agricultural wastes (SCB) under controlled conditions transformed it into valuable carbon nanostructures such as graphene oxide (GO) and carbon nanotubes (CNTs). We discovered that both GO and CNTs was acted like carriers for drugs for controllable drug release. This makes them ideal for creating drug delivery systems. In this study we used a muffle furnace to charr SCB for preparing GO and CNTs by eco-friendly, fast and cost-effective method. The sulfadiazine (SD) drug loading (DL%) was 91.70 and 57.00 %, respectively. For GO and CNTs. Istead of swallowing a pill that releases its entire dose at once, these carbon carriers can slowly release the medication over time, providing a more sustained and controlled effect. The study showed that CNTs were particularly good at holding onto drugs compared to GO. This makes them promising candidates for future drug delivery applications.Our DFT calculations proved these also.

1. Introduction

Amorphous solid dispersions (ASDs) are magic trick for drugs. They take poorly soluble drugs and disperse them, at the molecular level, within a polymer matrix. This matrix acts like a friendly host, enveloping the drug *molecules* and coaxing them to mingle with water (Budiman *et al.*, 2023; Pandi, *et al.*, 2020).

The world of medicine is constantly evolving, seeking ingenious ways to deliver drugs more effectively and efficiently. Enter the realm of nanomedicine, where materials smaller than a human hair hold the potential to revolutionize therapy. This is where graphene oxide (GO) and carbon nanotubes (CNTs), two superstars of the nanocrystal world, step onto the stage. Imagine GO as a flat sheet of honeycomb-like carbon atoms, while CNTs are rolled versions of the same material, resembling miniature tubes. These tiny titans possess unique properties that make them ideal candidates for amorphous solid dispersions (ASDs), a game-changing technology in drug delivery (Debnath *et al.*, 2021; Jampilek & Kralova, 2021). The high price of the carbon-based polymers fostered researchers to research on alternative polymers based on the eco-friendly and bio-degradable lignocellulosic materials (LCMs) (Tohamy *et al.*, 2022). Agricultural wastes can be easily recycled into worthy products and used in ASD. Sugarcane bagasse (SCB) is LCMs with various active sites (Tohamy, *et al.*, 2023).

* Corresponding author.
E-mail address: hebasarhan89@yahoo.com

https://doi.org/10.61856/6w30zq45

In this work, the synthesis and characterization of GO and CNTs from agro wastes were investigated. Furthermore, the obtained polymers have been applied in ASD formulation and sulfadiazine (SD) controlled release.

2. Methodology

2.1. Materials

Sugarcane bagasse (SCB) was obtained from Quena Paper Industry, Egypt. SCB was air-dried and subjected to homogenization to prevent compositional differences among batches. SCB was then grinded to a mesh size of 450 µ.

2.2. Methods

2.2.1. Preparation of GO

SCB was charred in a muffle with a ferrocene catalyst for 10 minutes (Tohamy, 2022).

2.2.2. Preparation of CNTs

5 g of carbon precursor (SCB) was added into a mixture solution containing 10% $Fe_2(NO)_3 \cdot 9H_2O$, 10% $Ni(NO)_3 \cdot 6H_2O$, and 5% $(Co(NO)_3 \cdot 3H_2O)$. Then, 10 wt.% of urea in 20 ml H_2O was added to the previous mixture under vigorous stirring for 1 hr. The mixture was transferred into a stainless-steel reactor and heated in an electrical muffle at 180 °C for 3 hr. The hydrochar product was filtrated and washed with H_2O. Afterward, it was dried. In the next step, a wetness impregnation of $Al(OH)_3$ with 5 wt.% $Fe_2(NO)_3 \cdot 9H_2O$, $Ni(NO)_3 \cdot 6H_2O$ solutions and heated at 750 °C for 2 hr. in an electrical muffle. The obtained hydrochar was ground with this catalyst at a mass ratio of 10:1 and placed in the stainless-steel reactor at 800 °C for 1 hr. After cooling, the product was washed with 5M of HNO_3 and H_2SO_4, then with hot H_2O and dried. The yields of CNTs from SCB was 4.77% (Tohamy *et al.*, 2022).

2.2.3. Preparation of ASD

Probe sonication of GO and CNTs (0.1025 g) was carried out separately in an aqueous solution (10 mL distilled water) for 2 min. The hydrophobic drug (sulfadiazine, 0.1025 g) was then added into the polymeric self-assemblies and, after sonication for another 2 min on ice, the drug was encapsulated within the hydrophobic core of the self-assemblies. The excess drug was then filtered via syringe filtration (El-Sakhawy *et al.* 2017).

2.3. Characterization and analysis

Fourier-transform infrared spectra were collected employing Mattson 5000 spectrometer (Unicam, United Kingdom) using the KBr disk method. While, the morphology of samples was performed by using scanning electron microscopy (SEM, Quanta-250) and transmission electron microscope (TEM, JEOL JEM-2100) at an acceleration voltage of 120 kV.

2.4. Carrying sulfadiazine (SD) on to the prepared GO and CNTs

SD carrying was carried out as following: 102.50 mg Of GO or CNTs was probe sonicated in 10 ml aqueous solution for 3 min, on ice, to form micelles. Then, SD drug (102.50 mg) was added into the GO or CNTs mixture. The excess SD was then filtered via syringe filtration. The obtained micelle solution was lyophilized in a freeze-drier system in order to obtain the GO or CNTs loaded SD (GO@SD or CNTs@SD) (El-Sakhawy *et al.,* 2017).

2.5. Drug loading (DL)

DL was performed as following: 0.1025 g of GO@SD or CNTs@SD was added to 10 ml of phosphate buffer (concentration 10% w/v, pH 7.4) and kept for 3 days to allow the complete SD drug extraction from GO@SD or CNTs@SD. After 3 days, this solution was diluted and the absorbance was measured at 240 nm. The absorbance obtained was substituted in the regression equation of the standard curve data, and the unknown experimental concentration (CSD) was determined:

$$DL_{\mathrm{SD}}\ (\%, w/w) = \frac{\text{Weight of SD in GO@SD or CNTs@SD}}{Weight\ of\ \text{GOor CNTs}}\ X\ 100$$

https://doi.org/10.61856/6w30zq45

2.6. SD release study (DR_{SD})

The DRSD of the SD from the GO@SD or CNTs@SD was determined by using a dialysis membrane (12000- 14000, AVWR Company).

The membrane was filled with 1.5 mL of phosphate buffer (pH 7.4), maintained at 37 ± 0.5 °C and stirred by a magnetic bar at 80 rpm for 6 h. The membrane was activated in diffusion media by soaking in phosphate buffer. A sample of a particular formulation, equivalent to 1.7 mg of GO@SD or CNTs@SD, were suspended in 1.5 ml of phosphate buffer (pH 7.4), then placed on the activated membrane and added to 20 ml of dissolution medium. At appropriate time intervals, 1 ml aliquots of the receptor medium were withdrawn and immediately replaced by equal volumes of the fresh receptor solution. These samples were analyzed spectrophotometrically at 316 nm (El-Sakhawy *et al.* 2017).

$$DR_{\mathrm{SD}}\ (\%, w/w) = \frac{\text{Release of SD}}{Total\ \text{SD drug}}\ X\ 100$$

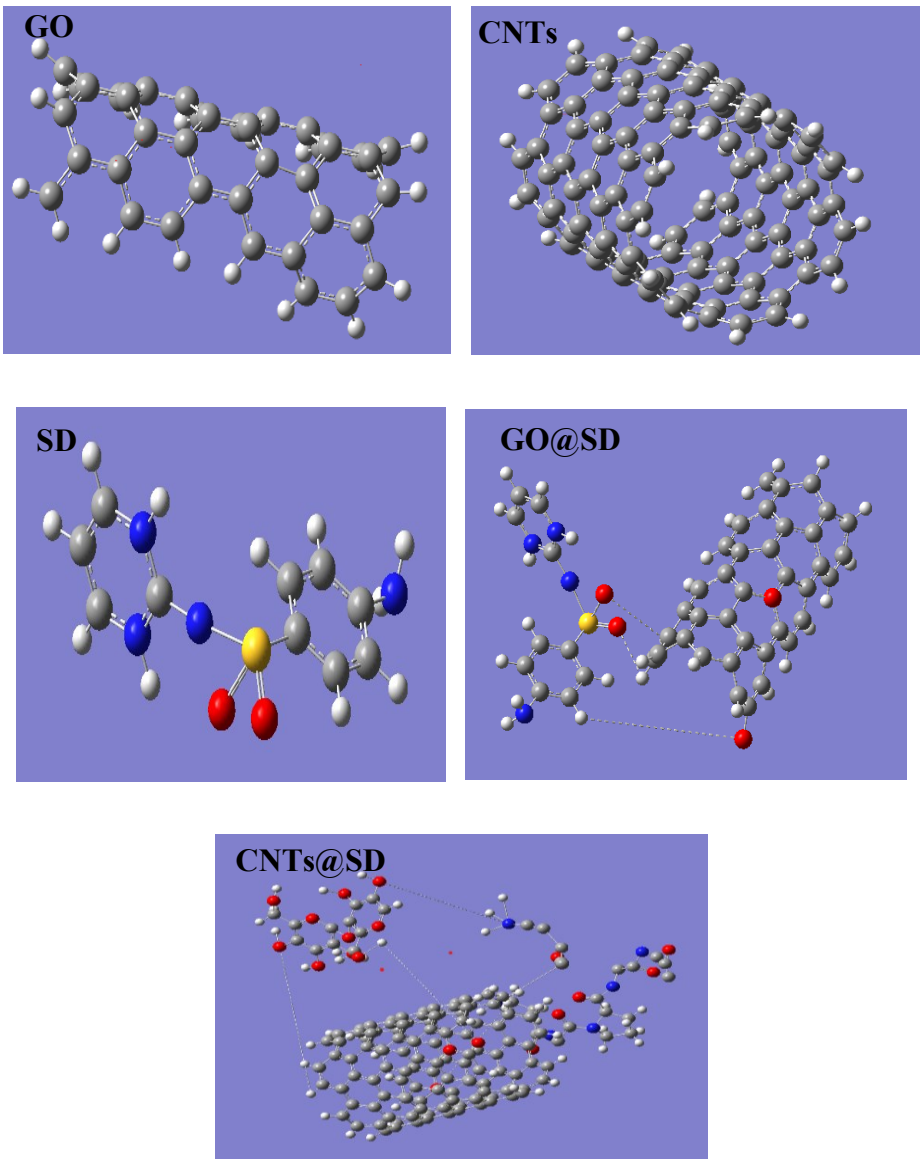

Figure 1. The optimized geometry of GO, SD, CNTs, GO@SD and CNTs@SD.

https://doi.org/10.61856/6w30zq45

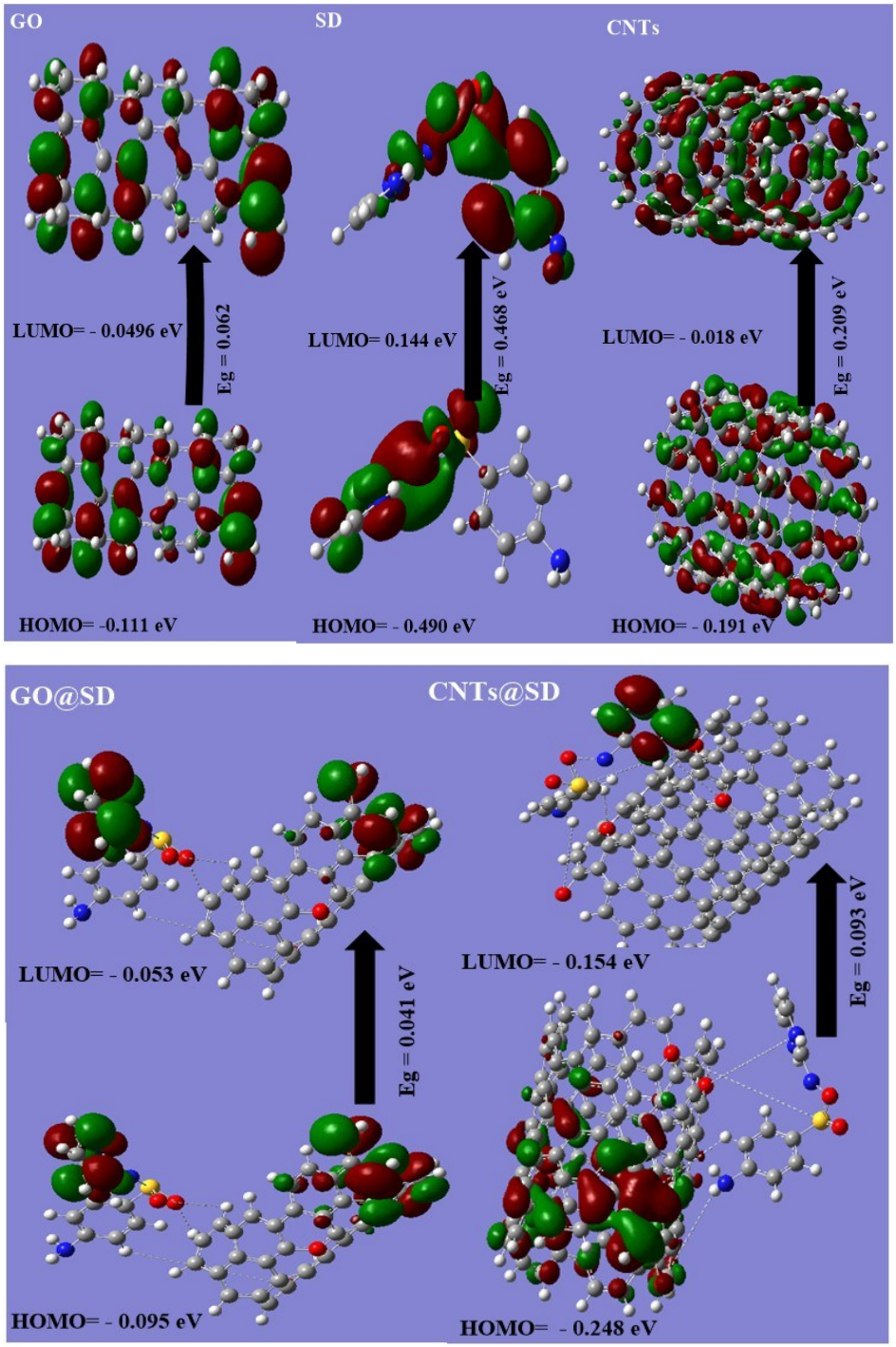

Figure 2. Gap energy (HOMO - LUMO) (eV) are calculated for hydrogel using DFT B3LYP/6-31G (d) and the molecular orbital's interaction between DAC, 4-AAP and chitosan.

https://doi.org/10.61856/6w30zq45

Table 1: The quantum chemical parameters of GO, CNTs, SD, GO@SD and CNTs@SD.

DFT	GO	SD	CNTs	GO@SD	CNTS@SD
E_{LUMO} (eV)	– 0.049	0.144	– 0.018	– 0.053	– 0.154
E_{HOMO} (eV)	– 0.111	– 0.490	– 0.191	– 0.095	– 0.248
E_T (au)	– 1440.78	–1143.343	–4532.84	–2694.440	1.604
E_g (eV)	0.062	0.468	0.209	0.041	0.093
μ (Debye)	0.031	6.1556	0.0023	31.016	42.154
η (eV)	0.031	0.234	0.104	0.020	0.046
χ (eV)	0.080	0.256	0.086	0.074	0.201
Pi (eV)	– 0.080	– 0.256	– 0.086	– 0.074	– 0.201
σ (eV)	32.102	4.272	9.528	48.076	21.344
S (eV)	16.051	2.136	4.764	24.038	10.672
ΔN max	– 2.592	– 1.096	– 0.827	– 3.586	– 4.306

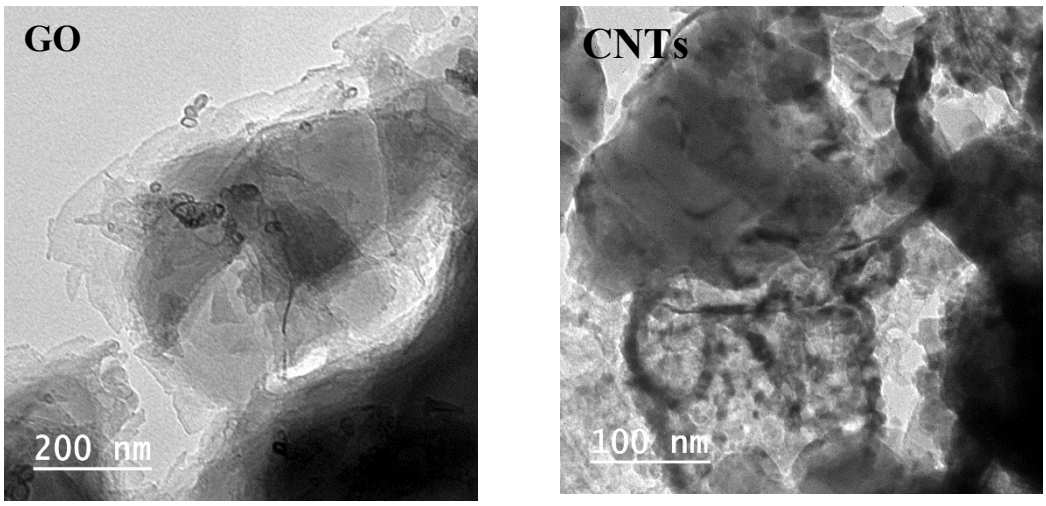

Figure 3. TEM analysis of GO and CNTs.

https://doi.org/10.61856/6w30zq45

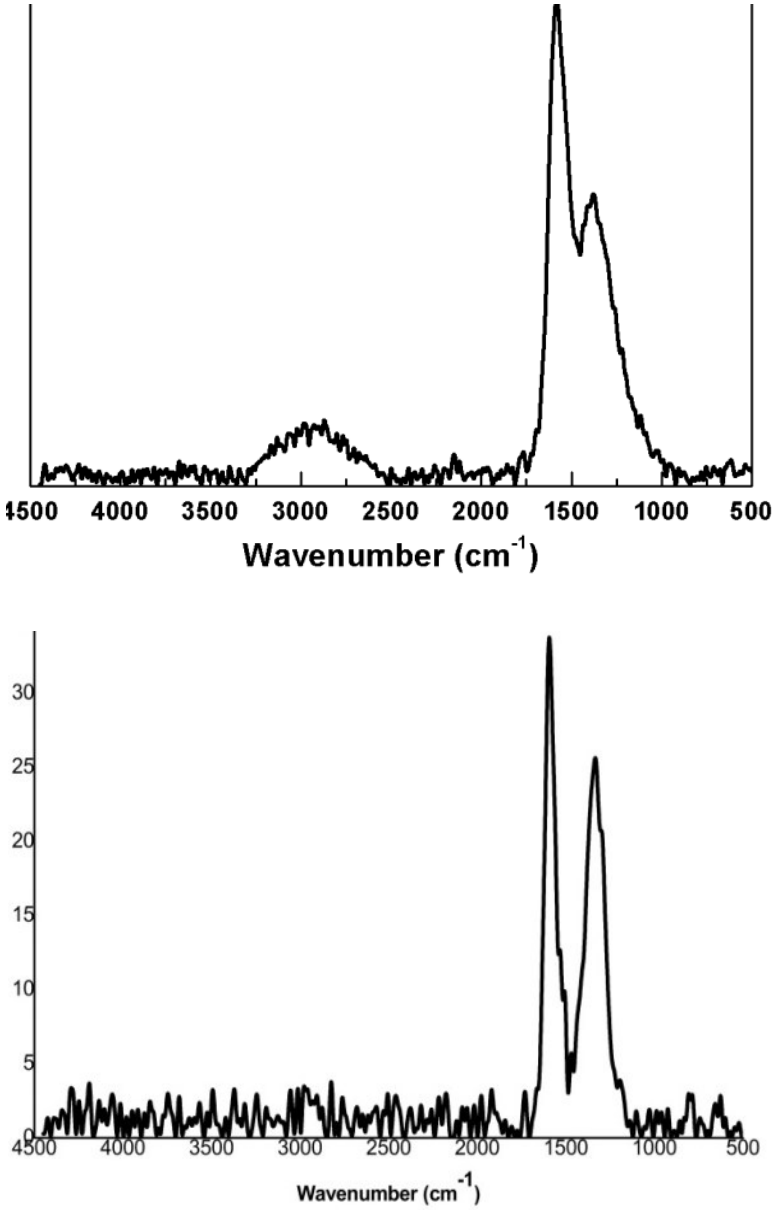

Figure 4. Raman analysis of GO and CNTs.

https://doi.org/10.61856/6w30zq45

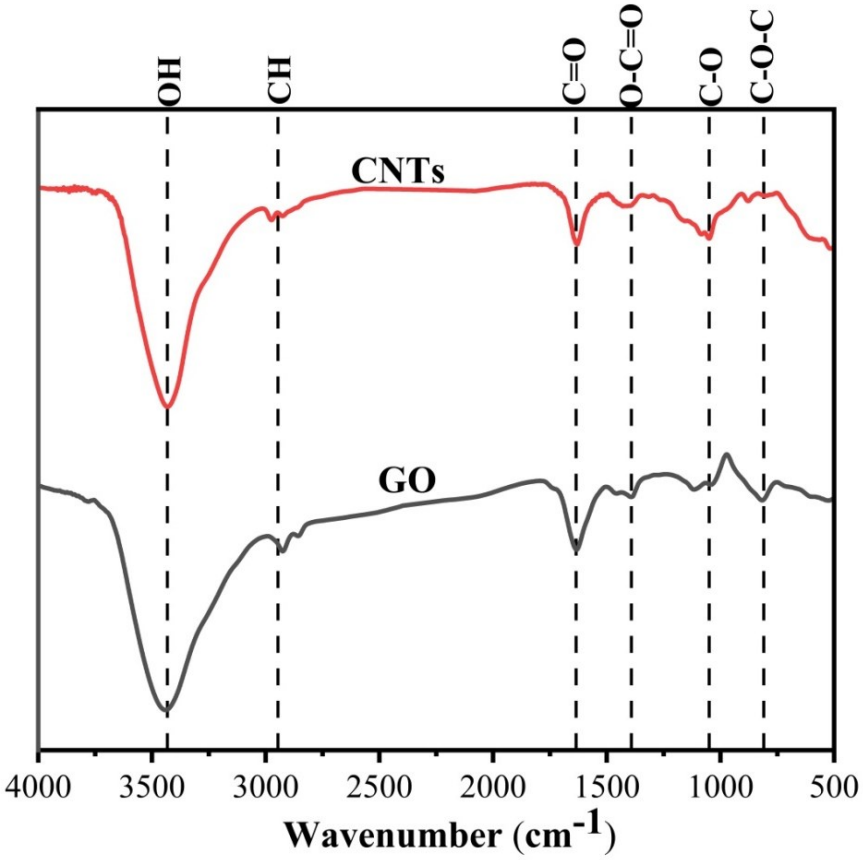

Figure 5. FTIR spectra of GO and CNTs.

Table 2: LOI and MHBS values for GO and CNTs.

Sample	MHBS ($\frac{A_{OH}}{A_{CH}}$)
GO	0.82
CNTs	0.86

https://doi.org/10.61856/6w30zq45

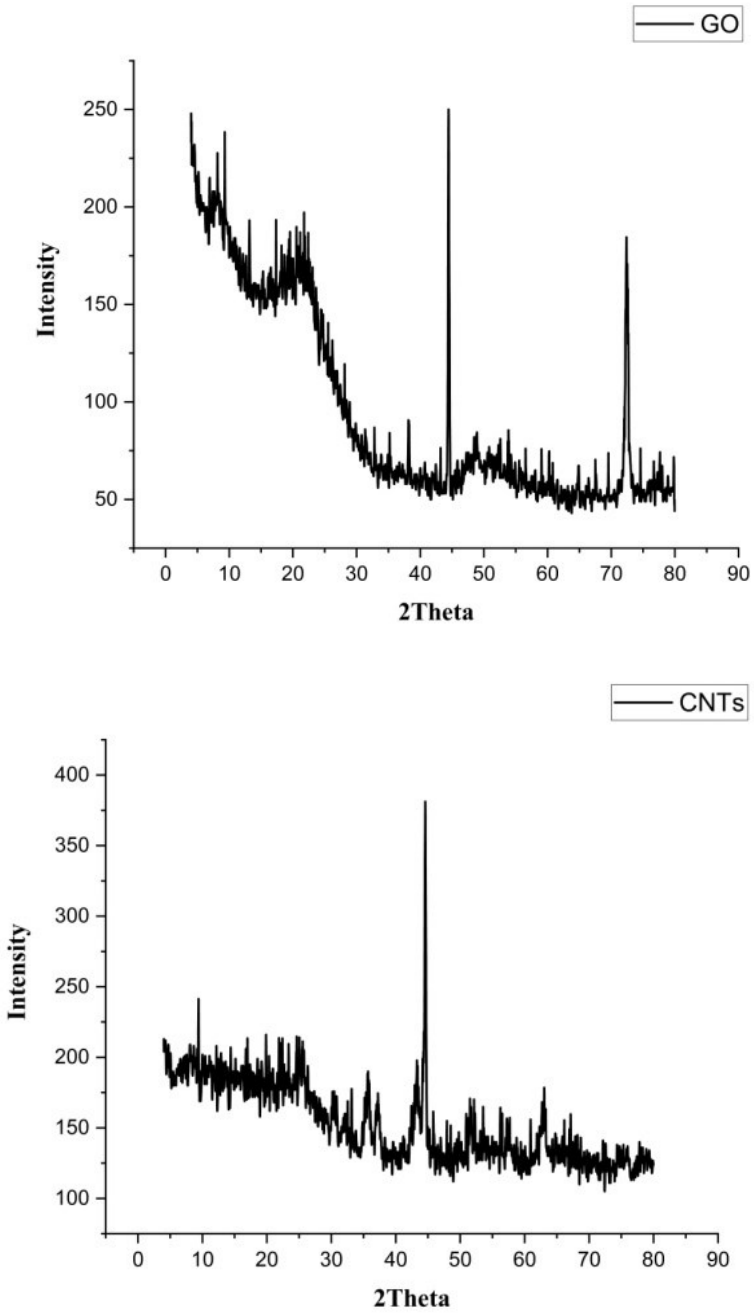

Figure 4. XRD of GO and CNTs.

https://doi.org/10.61856/6w30zq45

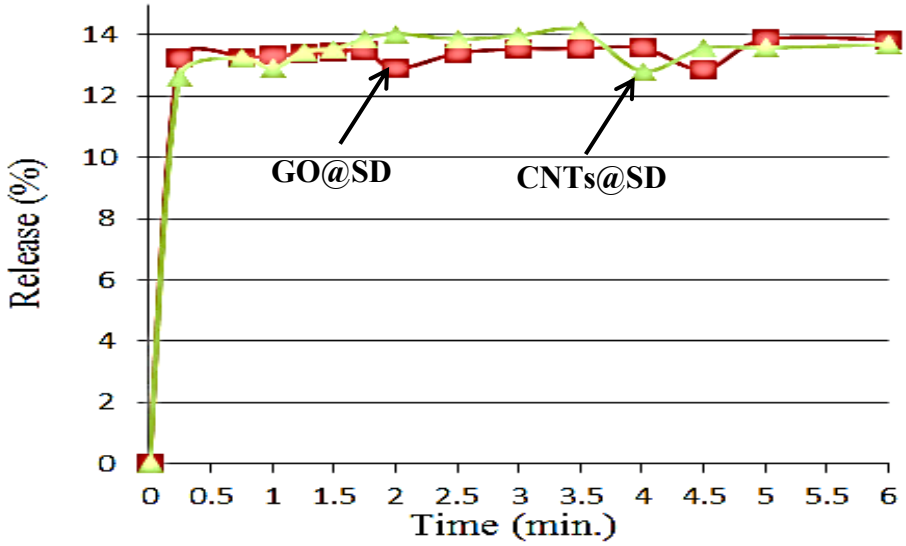

Figure 5. Release study from GO@SD and CNTs@SD.

2.7. Computational procedures

The Gaussian 09 W program was used to perform density functional theory (DFT) calculations with the hybrid functional B3LYP (Becke's three-parameter hybrid functional utilizing the BLYP correlation functional) with the 6-31G(d) basis set exhausted by the Berny technique. Different parameters were investigated via DFT calculations, including some of the optimized geometries and ground state energies, including total energy (E_T), the energy of the highest occupied MO E_{HOMO}, the energy of the lowest unoccupied MO E_{LUMO}, the energy gap (E_g), the dipole moment (μ), the absolute electronegativity (χ), the chemical potential (Pi), the absolute hardness (η), the absolute softness (σ), the global electrophilicity (ω), the chemical softness (S), and the additional electronic charge (ΔN_{max}).

$$E_{gap} = (E_{LUMO} - E_{HOMO})$$

$$\chi = \frac{-(E_{HOMO} + E_{LUMO})}{2}$$

$$\text{Pi} = -\chi$$

$$\eta = \frac{(E_{LUMO} + E_{HOMO})}{2}$$

$$\sigma = \frac{1}{\eta}$$

$$S = \frac{1}{2\eta}$$

$$\Delta N_{max} = \frac{-\text{Pi}}{\eta}$$

$$\omega = \frac{Pi^2}{2\eta}$$

3. Results and discussion

3.1 DFT computational calculations

DFT calculations were employed to study the stability of the GO, CNTs, SD, GO@SD and CNTs@SD. From Fig. 1 and Table 1, the results show the following:

– The GO@SD formulation is much softer (24.038 eV) than the GO alone (16.051 eV), while, CNTs@SD (10.672 eV) is much harder than GO@SD. This prove the high efficiency of GO@SD compared to CNTs@SD.

– From the calculations of the E_g, which represents the chemical activity of the HOMO–LUMO, the E_g, for GO@SD (0.041 eV) was lower than CNTs@SD (0.093 eV); demonstrating that charge transfer occurs much more within GO@SD, which in turn proves the strong chemical reaction between GO and SD. Consequently, the lowering of the HOMO–

https://doi.org/10.61856/6w30zq45

LUMO energy gap is essentially a consequence of the large stabilization of the LUMO due to the strong electron–accepting capability of the electron–acceptor group and influences the biological activity of the molecule (Fig. 2).

3.2. Morphological analysis

TEM analysis of GO revealed pure fluffy sheets. The CNTs revealed needles like CNTs bundles grow between GO (Figure 3). The calculated diameters of the obtained CNTs was 5.39 nm.

3.3. Raman analysis

Figure 2 shows a comparison of the Raman spectra of GO and CNTs. The G- bands located at 1582 cm^{-1} for GO is blue shifted to 1593 cm^{-1} for CNTs, proves the presence of more sp2 clusters on CNTs. The D- band is at 1378 cm-1 for GO and at 1333 cm^{-1} for CNTs. The ID/IG for GO and CNTs was 0.59 and 0.74, respectively, which confirms that CNTs are well-graphitized.

3.4 FTIR spectroscopy

The FTIR spectra of the prepared GO and CNTs show absorption bands between 3429–3441 cm-1 (OH), 2930–2974 cm-1 (CH), 1629–1634 cm-1 (C=O), 139–1395 cm-1 (O–C=O), 1045–1058 cm-1 (C–O), 812–872 cm-1 (C–O–C) (Figure 3). A shift in the OH bands of the GO from 3441 cm-1 to 3429 cm-1 for CNTs is mainly due to the strong H–bonding between CNTs (Misra *et al.*, 2006; Surekha, *et al.*, 2020). The calculated mean hydrogen bond strength (MHBS) proved that CNTs (i.e. 0.86) contain strong H–bonds compared to GO (i.e. 0.82) (Table 2).

3.5 XRD analysis

The XRD pattern revealed the known peaks of GO and CNTs with peaks at 2θ= 9.0 & 9.3 and 21.0 & 25.5° related to the (001) and (002) planes (Figure 4).

3.5 Drug loading and SD release study

After releasing the SD from the GO@SD and CNTs@SD, the amount of loaded SD was proportional to its concentration and could be determined at 240 nm. The DL calculation from GO@SD and CNTs@SD was 91.70 and 57.00 %, respectively. The GO@SD formulation was able to slow down the release of the SD drug compared to CNTs@SD. Figure 5 shows the release profile of the SD from the GO@SD and CNTs@SD.

4. Conclusions

The GO and CNTs were prepared from SCB at a muffle furnace by simple and eco-friendly method. The prepared materials were proved by Raman analysis which showed G and D bands ratios equal to 0.59 and 0.74 which aligned with GO and CNTs. In addition, the TEM analysis proved the fluffy sheets of GO and the needles of CNTs. From these we can say that we prepared GO and CNTs by a fast and eco-friendly method. These GO and CNTs were used to carry SD. They showed a DL 91.70 and 57.00 %, respectively. The GO@SD and CNTs@SD matrices were manufactured in this research paper showed an extended release profile over 6 hours.

Acknowledgements

The author acknowledges the National Research Centre and the Academy of Scientific Research and Technology (ASRT), Egypt, grant No. 9118 and the Czech Academy of Sciences, grant No. ASRT-22-01 through the Joint Bilateral Agreement project “Stimuli-responsive smart materials from agricultural wastes”, for financial support of the bilateral research activities.

References

Budiman, A., Handini, A. L., Muslimah, M. N., Nurani, N. V., Laelasari, E., Kurniawansyah, I. S., & Aulifa, D. L. (2023). Amorphous Solid Dispersion as Drug Delivery Vehicles in Cancer. Polymers, 15(16), 3380. https://doi.org/10.3390/polym15163380

Debnath, S. K., & Srivastava, R. (2021). Drug delivery with carbon-based nanomaterials as versatile nanocarriers: progress and prospects. Frontiers in Nanotechnology, 3, 644564. https://doi.org/10.3389/fnano.2021.644564

El-Sakhawy, M.., Salama, A., Kamel, S., & Tohamy, H. A. S. (2018). Carboxymethyl cellulose esters as stabilizers for hydrophobic drugs in aqueous medium. Cellul Chem Technol, 52(9–10), 749-757.

https://doi.org/10.61856/6w30zq45

Jampilek, J., & Kralova, K. (2021). Advances in drug delivery nanosystems using graphene-based materials and carbon nanotubes. Materials, 14(5), 1059. https://doi.org/10.3390/ma14051059

Misra, A., Tyagi, P. K., Singh, M. K., & Misra, D. (2006). FTIR studies of nitrogen doped carbon nanotubes. Diamond and related materials, 15(2-3), 385-388. https://doi.org/10.1016/j.diamond.2005.08.013

Pandi, P., Bulusu, R., Kommineni, N., Khan, W., & Singh, M. (2020). Amorphous solid dispersions: An update for preparation, characterization, mechanism on bioavailability, stability, regulatory considerations and marketed products. International journal of pharmaceutics, 586, 119560. https://doi.org/10.1016/j.ijpharm.2020.119560

Surekha, G., Krishnaiah, K. V., Ravi, N., & Suvarna, R. P. (2020). FTIR, Raman and XRD analysis of graphene oxide films prepared by modified Hummers method. Paper presented at the Journal of Physics: Conference Series. https://doi.org/10.1088/17426596/1495/1/012012

Tohamy, H.-A. S. (2022). Reinforced modified carboxymethyl cellulose films with graphene oxide/silver nanoparticles as antimicrobial agents. Egypt J. Chem, 65, 509-518. https://doi.org/10.21608/ejchem.2022.157801.6834

Tohamy, H.-A. S., El-Sakhawy, M., & Kamel, S. (2022). Carbon Nanotubes from Agricultural Wastes: Effective Environmental Adsorbent. Egyptian Journal of Chemistry, 65(131), 437-446. https://doi.org/10.21608/ejchem.2022.123337.5511

Tohamy, H.-A. S., El-Sakhawy, M., & Kamel, S. (2023). Microwave-assisted synthesis of amphoteric fluorescence carbon quantum dots and their chromium adsorption from aqueous solution. Scientific Reports, 13(1), 11306. https://doi.org/10.1038/s41598-023-37894-4